This ICCV2013 paper is the Open Access version, provided by the Computer Vision Foundation.
The authoritative version of this paper is available in IEEE Xplore.

A Flexible Scene Representation for 3D Reconstruction Using an RGB-D Camera

Diego Thomas
National Institute of Informatics
Chiyoda, Tokyo, Japan
diego_thomas@nii.ac.jp

Akihiro Sugimoto
National Institute of Informatics
Chiyoda, Tokyo, Japan
sugimoto@nii.ac.jp

Abstract

Updating a global 3D model with live RGB-D measurements has proven to be successful for 3D reconstruction of indoor scenes. Recently, a Truncated Signed Distance Function (TSDF) volumetric model and a fusion algorithm have been introduced (KinectFusion), showing significant advantages such as computational speed and accuracy of the reconstructed scene. This algorithm, however, is expensive in memory when constructing and updating the global model. As a consequence, the method is not well scalable to large scenes. We propose a new flexible 3D scene representation using a set of planes that is cheap in memory use and, nevertheless, achieves accurate reconstruction of indoor scenes from RGB-D image sequences. Projecting the scene onto different planes reduces significantly the size of the scene representation and thus it allows us to generate a global textured 3D model with lower memory requirement while keeping accuracy and easiness to update with live RGB-D measurements. Experimental results demonstrate that our proposed flexible 3D scene representation achieves accurate reconstruction, while keeping the scalability for large indoor scenes.

1. Introduction

The fine 3D reconstruction of large indoor scenes from RGB-D measurements is of wide interest for the computer vision community, with various potential applications. For example, 3D models of indoor scenes can be used in serious games or indoor space organization. With recent efforts on developing inexpensive depth sensors such as the Microsoft Kinect camera or the Asus Xtion Pro camera (also called RGB-D cameras), capturing depth information in indoor environments becomes an easy task. This new set-up opens new possibilities for 3D reconstruction, and several softwares have been already proposed to realize live 3D reconstruction using RGB-D cameras.

In general, the live 3D reconstruction process can be divided into 4 steps: (1) RGB-D measurement acquisition; (2) camera tracking; (3) integration (or fusion) of aligned RGB-D measurements and (4) 3D modeling (3D textured mesh generation for example). The objective is then to carry out these tasks with both computational efficiency and high accuracy. Computational speed is important because we expect to capture many depth images (30 fps for the Kinect camera), so each image needs to be processed quickly in order to process the full sequence in a reasonable time. Even for an off-line application, the amount of data that is processed at each iteration imposes the use of graphic cards with large parallel computational power, but available memory space is limited. On the other hand, accuracy of the output 3D model is also important; in particular when we want it to be usable in games, simulations or visualization tasks. Using all available measurements including color is expected to achieve the accurate 3D reconstruction.

A standard approach to 3D reconstruction using RGB-D cameras is to employ a frame-to-frame strategy [8, 10, 11]. Each incoming frame is aligned to its previous frame, then newly aligned data are integrated into a global model (using surfels [15] for example), which is triangulated in a final post-process (using poisson surface reconstruction [12] for example). A crucial limitation of this strategy comes from the frame-to-frame error propagation, which can lead to significant errors at the end of the sequence. This becomes fatal when the scale of the scene is large. A loop closure algorithm may reduce the propagated error if a loop exists. However, its effectiveness is limited as the whole sequence has to be processed again to fuse all measurements after correcting the estimated camera trajectory and, moreover, loops are not always available. In this approach, only the current and previous frames are loaded on the GPU memory for camera tracking and, therefore, the GPU memory use is low and tracking is fast.

Another approach to 3D reconstruction is to use the frame-to-global-model strategy, which has been proven effective with KinectFusion [13] and its extensions [14, 16, 21]. In this strategy, a single high-quality global 3D model is updated along with live depth measurements, where the global model is represented as a signed distance function that is discretized into a volume covering the scene to be reconstructed. Incoming depth images are then aligned to high-quality predicted depth images generated from the global model. Using a global model allows to reduce the error propagation, however, the volumetric representation of the scene is highly memory consuming. As a consequence, most of the GPU memory space is used to update the global model and generate depth images. Thus additional operations on the GPU that require significant memory (such as SIFT-GPU) are not executable. Feature appearance based alignment methods, for example, cannot be used to augment the ICP based pose estimation. Accordingly, without rich geometric features in RGB-D image sequences, the method does not work well. In addition, the method is not well scalable to large scenes. Extensions of KinectFusion have been proposed where the volume is moved along with the camera to reconstruct large indoor scenes. However, rich geometric features are still required for camera tracking. Existing volumetric methods cannot deal with an RGB-D image sequence whose part has poor geometric features (like when passing through a corridor for example).

In this paper, we introduce a new 3D scene representation using a set of planes[1] that requires low memory use and, nevertheless, realizes accurate and efficient 3D reconstruction of a scene from an RGB-D image sequence, even when some parts of the sequence have poor geometric features. In this work, we focus on reconstructing indoor scenes because current RGB-D sensors work only indoors. The main idea is to represent a static scene as a set of planes to each of which we attach as its attributes three images describing the local geometry and color. This representation is flexible in that we can easily build and update the scene representation and more importantly, with the attributes, we can always recover the full 3D information of the scene while reducing required memory. Figure 1 illustrates our proposed 3D representation for an indoor scene.

The low memory use required to maintain our 3D scene representation allows us to use both geometry and color for camera tracking with standard graphic cards. In addition, thanks to our representation, the organization of data is over 2D grids on different planes, which gives us a quadrangulation (*i.e.* triangulation with quads) of the global 3D model effortlessly. We can thus generate high-quality dense depth and color images that can be used into the frame-to-global-model registration framework. Moreover, our 3D scene representation enables us to directly output roughly segmented dense 3D textured meshes from a large sequence of RGB-D images, even when parts of the sequences lack in rich geometric features. Experimental results confirm effectiveness of our proposed representation, showing accurate 3D reconstruction of scenes.

[1]In this paper we use planes only for simplicity, but the same approach can be used straightforwardly with other parametric shapes such as spheres, cylinders or cones, once they are detected from the image sequence.

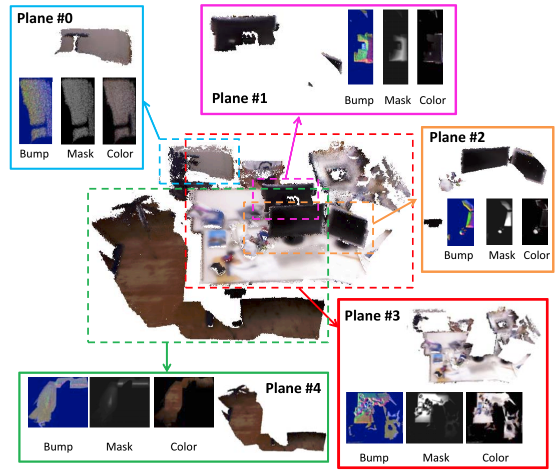

Figure 1. The proposed 3D representation for an indoor scene.

2. Related work

A successful approach to 3D reconstruction using RGB-D cameras is the frame-to-global-model strategy. Methods using such a strategy build and update a global 3D model with higher resolution than that of input depth images in an online manner along with live measurements.

Weise *et al.* [20] proposed to build a global model using surfels [15] and align successive frames to the global model using GICP [17] (extension of ICP [3] where the point-to-plane metric is used instead of the point-to-point metric). Using triangular meshes for a global model requires considerable efforts to guarantee the integrity and quality of the mesh topology after adding, updating, or removing any vertices. As addressed in [20], however, the use of surfels has the advantage that it can be easily updated with live measurements while keeping consistency of the global model. A robust algorithm is also proposed to detect registration failures. One drawback of this method is that the surfel representation is relatively sparse compared with captured depth images, which degrades the accuracy of registration results. Moreover the memory space required to maintain the surfel representation for large scenes is not practical.

Recently, Newcombe *et al.* [13] proposed KinectFusion where the global 3D model is represented as a signed distance function that is discretized into a volume covering a scene to be reconstructed. Incoming depth images are then aligned to a high-quality predicted depth image generated from the global model. Improvement of KinectFusion to better handle input noise was proposed by Nguyen *et al.* [14]. The advantage of using a volumetric representation of the scene is that dense depth images can be rendered for a given camera position. Moreover, updating the volume is easy and fast thanks to the GPU. The major drawback is, on the other hand, scalability. Namely, for a given resolution, the data size for the volume becomes too large and memory consuming when the target scene becomes large.

Extensions of KinectFusion to a large scene have been proposed where the volume is moved along with the tracked camera motion. Roth *et al*. [16] proposed a method to automatically translate and rotate the volume in space as the camera moves. The volume is remapped into a new one by the Truncated Signed Distance Function (TSDF) interpolation whenever sufficient camera movement is observed. The objective of this work is to output fine camera tracking with a local map of the environment. As a consequence, points that leave the volume are lost and the method can not generate the complete reconstructed scene. Similarly, Whelan *et al*. [21] introduced Kintinuous, proposing a method to identify points that leave the KinectFusion volume and incrementally add them into a triangular mesh representation of the scene. Available implementation that can be found in the PCL [1] allows even to re-use existing data when moving the volume. However, rich geometric features in the RGB-D image sequence are required for accurate scene reconstruction. When a scene does not have rich geometric features, this method fails in tracking the camera motion, resulting in poor reconstruction.

Much recently, Zeng *et al*. [22] and Chen *et al*. [6] proposed an octree-based fusion method to compress the volumetric TSDF representation of the scene. At the same time, Zhou *et al*. [23] proposed to use local volumes around points of interest and Henry *et al*. [9] proposed to segment the scene into planar patches and use 3D TSDF volumes around them to represent the 3D scene. By contrast, our proposed method requires only three 2D images for each plane to model the scene, which allows more compact representation of the scene.

As the size of the scene to be reconstructed becomes large, representing the whole scene using clouds of points or volumes becomes unpractical. The more points that compose the scene exist, the heavier the post processing such as triangulation or texturing becomes. In this paper we propose a scene representation that allows to directly build roughly segmented 3D textured meshes from an RGB-D image sequence.

3. Scene representation using planes

For 3D scene reconstruction using RGB-D cameras, how to represent the target scene is of crucial importance. The representation should be (1) compact, so that the user can reconstruct large scenes, (2) accurate for fine reconstruction, (3) easy to update with live measurements for fast processing, and (4) capable of predicting dense high-quality RGB-D images for accurate camera tracking. To the best of our knowledge, there is no 3D representation that satisfies these four requirements, which motivates us to introduce a new flexible 3D scene representation.

We reason that parametric shapes such as planes can be used to describe an indoor scene because it is mainly composed of man-made objects (such as table, wall and storage for example), with rather simple shapes. We thus propose to represent a scene as a set of planes (again only for simplicity) having attributes. To each plane[2] detected in the scene, we attach as its attributes three 2D images in addition to information that identifies the plane (planar patch).

The three images are a three-channel Bump image, an one-channel Mask image and a three-channel Color image; these three images encode the geometric and color details of the scene. The Bump image encodes the local geometry around the plane. For each pixel, we record in the three channels the displacement of the 3D point corresponding to the pixel from the lower left-corner of the pixel. The Mask image encodes the confidence for the accumulated data at a point and the Color image encodes the color of each point.

The Bump image encodes the local geometry, which allows us to accurately represent the geometry of the 3D scene while using less memory. This satisfies the first two requirements. In addition, adding, removing or updating points is executed easily and efficiently, because we are manipulating 2D images. Therefore we satisfy the third requirement. Last but not least, the organization of points over 2D images gives a natural quadrangulation for the reconstructed scene. We choose quads rather than triangles because the quadrangulation is a natural meshing for a 2D grid (also the number of quads becomes smaller than that of triangles when generating meshes). We can thus render 3D textured meshes from an estimated camera pose to obtain a high-quality *dense* predicted RGB-D image from the global model using 3D renderers such as OpenGL. Our proposed 3D representation thus satisfies the fourth requirement as well.

3.1. Plane detection

We detect different planes that decompose the target scene by modifying the method proposed in [4] (we employ the Floyd-Warshall algorithm [7] to detect local maxima). We choose this voting strategy rather than another one such as RANSAC [18], Generalized PCA [19] or Robust PCA [5] because it is known to be fast with decent accuracy. Note that for our 3D representation the accuracy of detected plane parameters is not critical. Any errors that arise during the plane detection will be compensated by the Bump image.

For each point in a given depth image, we first compute its normal vector and generate a histogram of normals from the depth image. Namely, each point votes in the bin corresponding to its normal vector. Then, the bins with sufficient votes are detected and connected bins are merged using the Floyd-Warshall algorithm [7]. The median normal vector for each connected class is then computed. We thus ob-

[2] Since a visible region of a plane in the scene has a finite size, a planar patch may be more appropriate, however, we use the word plane for simplicity. We remark that, in our method, each plane is identified by its plane equation and a bounding box.

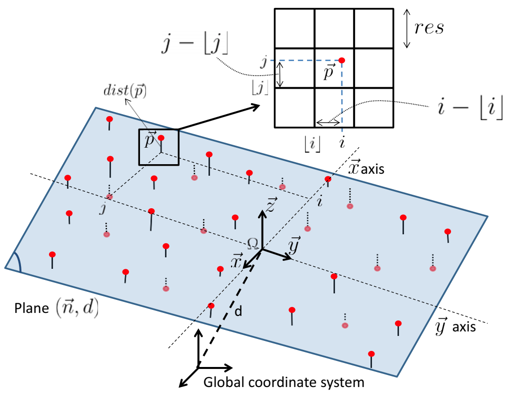

Figure 2. A simple example for the Bump image computation.

tain a set of normals for the depth image as well as lists of points to each of which a normal vector in the set is attached. Thereafter, for each normal vector in the set, we compute for each point in its corresponding list the plane that passes the point and that has the normal vector and then compute the distance d_{origin} of the origin from this plane. Each point in the list then votes in the bin of a distance histogram corresponding to d_{origin}. Again, bins with sufficient votes are identified and connected bins are merged using the Floyd-Warshall algorithm [7]. By identifying the median of distances for each connected class, we finally obtain a set of plane parameters for the input depth image.

When a plane has been visible a sufficient number of times, we refine the plane parameters (in the experiments, we refined plane parameters when the plane has been visible twice, 20 times and 80 times). After obtaining new plane parameters, we recompute all attributes of the plane.

3.2. Bump, Mask and Color images

The Bump image, encoded as a three-channel 16 bits image, represents the local geometry of the scene around a plane. For a given plane, the Bump image is obtained by identifying points around the plane and projecting them onto the discretized plane. The three values of a pixel in the Bump image encode the exact 3D position of the point corresponding to the pixel in the global coordinate system. For the Bump image, only a few bytes are required to record the position of a 3D point regardless of the size of the scene, which makes our 3D model require lower memory cost.

We describe more in detail how to obtain the Bump image and how to recover the 3D coordinates of 3D points using a simple example. Figure 2 depicts our simple example, where 3D points are randomly distributed around a plane defined by $(\vec{n}, d)$, where $\vec{n}$ is the normal vector of the plane and d is the distance of the plane from the origin. Our objective is then to compute the Bump image for the plane and to accurately recover the set of 3D points using only the plane parameters and the computed Bump image.

We define an arbitrary orthonormal coordinate system $(\vec{x}, \vec{y}, \vec{n})$ for the plane, with the origin $\vec{\Omega}$ being the projection onto the plane of the origin of the global coordinate system. The $\vec{x}$ and $\vec{y}$ axes are obtained as follows:

$$\begin{cases} \vec{x} = \frac{[-n[1], n[0], 0]}{\|\vec{x}\|} \text{ if } n[0] > n[1] \text{ and } n[0] > n[2], \\ \vec{x} = \frac{[0, -n[2], n[1]]}{\|\vec{x}\|} \text{ if } n[1] > n[0] \text{ and } n[1] > n[2], \\ \vec{x} = \frac{[n[2], 0, -n[0]]}{\|\vec{x}\|} \text{ if } n[2] > n[0] \text{ and } n[2] > n[1], \end{cases}$$

where $n[0]$, $n[1]$ and $n[2]$ stand for the first, second and third components (respectively) of $\vec{n}$. Then the $\vec{y}$ axis is obtain as the cross product of $\vec{n}$ and $\vec{x}$. With this coordinate system for the plane and a given resolution res, we can discretize the plane into pixels of size res.

Let us now consider a 3D point $\vec{p}$. From the plane parameters, we can compute the distance $dist(\vec{p})$ of the 3D point from the plane. If $\|dist(\vec{p})\| > \epsilon$, with ϵ being a threshold defining the width for the plane (we used $\epsilon = 10\text{cm}$ in the experiments), then $\vec{p}$ does not appear in the Bump image. Otherwise, we project $\vec{p}$ onto the plane to obtain its 2D coordinates $\vec{\pi}(\vec{p})$ in the plane. If $\vec{\pi}(\vec{p})$ is outside of the bounding box, then $\vec{p}$ does not appear in the Bump image. With the origin $\vec{\Omega}$ and the resolution res, we obtain the coordinates $[i, j]$ of $\vec{p}$ in the Bump image as $[i, j] = [\frac{\vec{\pi}(\vec{p})[0] - \Omega[0]}{res}, \frac{\vec{\pi}(\vec{p})[1] - \Omega[1]}{res}]$. We then discretize the coordinates to have pixel indices for $\vec{p}$: $[\lfloor i \rfloor, \lfloor j \rfloor]$. In this way, we identify the pixel of the Bump image that corresponds to $\vec{p}$. We encode in the Bump image deviation caused by the discretization process together with the distance of $\vec{p}$ from the plane so that we can exactly recover the 3D position of $\vec{p}$. Namely, $Bump([\lfloor i \rfloor, \lfloor j \rfloor]) = [i - \lfloor i \rfloor, j - \lfloor j \rfloor, dist(\vec{p})]$. We remark that to record the values of $Bump([\lfloor i \rfloor, \lfloor j \rfloor])$ in 16 bits, we employed affine scaling and casting to integer. However we keep the values as they are in the remaining of this paper for clarity.

On the other hand, computing the 3D positions of points is easy. Given a plane and its Bump image, it is straightforward to compute the exact position of a point corresponding to a pixel (k, l) in the global 3D coordinate system.

$$\begin{aligned} \vec{p}(k, l) = \vec{\Omega} + (res(\text{Bump}(k, l)[0] + k))\vec{x} + \\ (res(\text{Bump}(k, l)[1] + l))\vec{y} + \text{Bump}(k, l)[2]\vec{n}. \end{aligned} \quad (1)$$

The Mask image encodes the confidence for 3D points. This allows us to perform a running average when integrating live measurements and also to eliminate erroneous measurements. The values of the Mask image are initialized when generating the Bump image. A pixel in the Mask image is set to 1 if a point is projected onto the same pixel in the Bump image, it is set to 0 otherwise. The Mask image is then updated with live measurements as explained in Section 4.2. The Color image takes the RGB values of the points that are projected into the corresponding pixel in the Bump image. We can thus recover color information of 3D points as well.

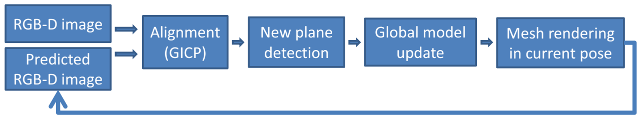

Figure 3. The pipeline of our proposed method.

4. Scene reconstruction

The implicit quadrangulation given by the 2D discretization of each plane allows us to maintain our 3D mesh representation of the scene. The global mesh is used to render a dense and high-quality predicted depth image (see Section 4.2) to accurately align incoming depth images. Our scene representation is then updated with aligned live measurements, and newly detected planes, if any, are added as the camera moves through the scene. The pipeline of our proposed method is illustrated in Fig. 3.

4.1. Camera tracking

Accurately tracking the camera is of crucial importance for any 3D reconstruction method. As proposed in KinectFusion [13], we also employ the linearized version of the GICP [17] because it is fast with sufficient accuracy when using RGB-D sensors. Thanks to low memory use for our scene representation, we still have the GPU memory space available enough to combine the linearized GICP with the SIFT-GPU [2] algorithm in the same way as [10]. This allows us to reconstruct scene even when parts of the RGB-D image sequence are poor in geometric features.

For the linearized GICP to work well, a key issue is to align incoming frames with a dense and high-quality predicted depth image. Thereafter, the dense point matching allows robust and accurate registration. For this reason, directly projecting all the points of the global model into the current camera plane is not appropriate. This is because (1) parts of the scene that are close to the camera would produce relatively sparse depth information and (2) handling occlusions would require significant efforts. Instead, we take advantage of the natural quadrangulation given by the 2D image discretization to render a depth image using meshes.

From the Mask image of each plane, we identify correct quads (*i.e.* quads that have positive mask values at their four summits). This straightforwardly gives us a quadrangulation for each plane (vertices are computed using Equation (1)), which can be quickly rendered into the current camera plane using a 3D renderer such as OpenGL. Note that for a given camera pose, only planes intersecting with the perspective frustum of the current camera pose are rendered, which eases computation.

Using the rendered color image is not good for SIFT matching. This is because small errors in camera tracking, misalignments between depth and color images and motion blur tend to blur the color image, which is fatal when extracting and matching SIFT features. To avoid this problem, we use the color image of the previous frame superimposed over our predicted depth image to align the current frame.

4.2. Updating model with live measurements

With the estimated camera pose, and the live RGB-D measurements, we can now update and refine our 3D scene representation. We reason that RGB-D sensors such as the Microsoft Kinect camera have strong noise in the viewing direction. Therefore we propose to always fuse live measurements in the viewing direction of the camera. The currently aligned depth image is merged with the predicted depth image using a rendered Mask image. The newly obtained 3D points are then projected onto different planes and the attributes of each plane are updated by replacing mask, color and bump values with newly computed ones (if available). In contrast, straightforwardly projecting live measurements onto the different planes and then updating the mask, color and bump values at the projected pixel does not give nice results. This is because the point corresponding to a pixel of the input depth image and the point represented at the projected pixel in the plane do not likely represent the same point at the surface.

Let us consider a model RGB-D image D_M rendered at the current camera pose, and a newly acquired RGB-D image D_T. We also render a Mask image $Mask$ in the same way as for D_M but by replacing the RGB values of vertices with the mask values. This allows us to perform a running average. Thereafter we merge the two RGB-D images using the Mask image and visibility constraints.

Let $[k,l]$ be a pixel and D_{merged} be the merged RGB-D image. Then $D_{merged}[k,l]$ is computed as follows:

$$\begin{cases} D_{merged}[k,l] = D_M[k,l] \text{ and } \mathrm{Mask}[k,l] = \mathrm{Mask}[k,l] \\ \quad \text{if } D_T[k,l] \text{ is not available} \\[1ex] D_{merged}[k,l] = D_T[k,l] \text{ and } \mathrm{Mask}[k,l] = 1 \\ \quad \text{if } D_M[k,l] \text{ is not available} \\[1ex] D_{merged}[k,l] = D_T[k,l] \text{ and } \mathrm{Mask}[k,l] = 1 \\ \quad \text{if } D_M[k,l] > D_T[k,l] + \delta \text{ (occlusion)} \\[1ex] D_{merged}[k,l] = D_M[k,l] \text{ and } \mathrm{Mask}[k,l] = \mathrm{Mask}[k,l] - 1 \\ \quad \text{if } D_M[k,l] < D_T[k,l] - \delta \text{ (visibility violation)} \\[1ex] D_{merged}[k,l] = \frac{D_T[k,l] + \mathrm{Mask}[k,l] \times D_M[k,l]}{\mathrm{Mask}[k,l]+1} \\ \quad \text{and } \mathrm{Mask}[k,l] = \mathrm{Mask}[k,l] + 1 \text{ otherwise} . \end{cases}$$

The threshold δ is used to check visibility violations and occlusions (we used $\delta = 10$ cm in the experiments). Note that color and depth values are merged similarly.

From the merged RGB-D image we can compute a new set of 3D points and record them into the attributes of each plane. Each point is first projected onto its corresponding plane. Then, for a point $\vec{p}$, if the mask value at the projected pixel is smaller than that of $\vec{p}$, then mask, color and bump values are all replaced by the newly computed values for the point $\vec{p}$. Note that if the mask values are the same, then we record the values of the point closest to the plane.

All points that do not belong to any existing planes are kept in a residual image from which new planes are detected. With the updated 3D scene representation, we can now proceed to the next frame. We set the RGB values of D_{merged} to those of D_T and use the obtained D_{merged} as the predicted RGB-D image for camera tracking.

Resizing planes From a single depth image, only some parts of planes are visible in general (like the ground for example). It is not possible to know the complete size of a plane right after detecting it. Therefore, we dynamically resize each plane (*i.e.* its bounding box) with live measurements. To do so, we use an arbitrary resizing step s ($s = 32$ pixels in the experiments). At each iteration, we evaluate whether points are added close to the boundary (closer than s). If added, we extend the size of the bounding box by s in the corresponding direction (for example, if points are close to the left boundary, then the bounding box's size is increased in the left direction). The information for the bounding box is updated accordingly to the new one and the Mask, Color and Bump images are-computed.

Merging planes Because of the noise in the depth images, false planes may be detected. However, since the Bump image records exact 3D point positions, after refining the plane parameters (see Section 3.1), the plane equation becomes correct. Then multiple planes may represent the same parts of the scene, which must be avoided. We identify such planes by computing the intersection of the bounding boxes of planes having similar parameters. If two planes have non-empty intersection between their bounding boxes, then the two planes are merged. To do so, we identify the parameters $(\vec{n}, d)$ and $(\vec{x}, \vec{y})$ of the largest plane and compute the union of the two bounding boxes of the largest plane and a plane to be merged in order to create the bounding box of the merged plane. Thereafter, points from the two planes are projected onto the merged plane with their respective color and mask values. Note that if two points project onto the same pixel in the merged plane, only the one with the maximum mask value is kept. The visibility of the merged plane is set to the one of the largest plane.

5. Experimental results

To demonstrate the effectiveness of our proposed method, we evaluated our algorithm using data that we captured using the Microsoft Kinect camera. We compared results by our method with those obtained using the KinFuLargeScale whose code is available in the PCL [1]. We

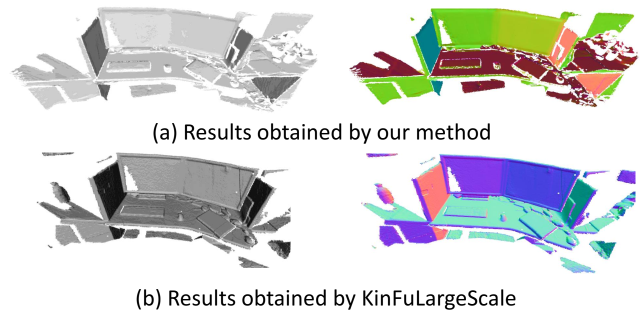

Figure 4. Results obtained with our method and KinFuLargeScale (untextured mesh on the left and normal image on the right).

also demonstrate the usefulness of our proposed method to tackle RGB-D image sequences whose parts do not have rich geometric features. All scenes were captured at 30 fps. For all results obtained by our method, we used a resolution of 0.4 cm for the attribute images and a threshold of 0.5 cm for the RANSAC outlier removal used after running the SIFT-GPU matching algorithm [2].

We evaluate the accuracy of our method to reconstruct an indoor scene in fine details by comparing our results with those by KinFuLargeScale. We captured a small scene with rich geometric features, which is an ideal situation for KinFuLargeScale. Figure 4 shows the results obtained with this data by our method and by KinFuLargeScale. On the left side of the figure, we show the reconstructed 3D mesh without color and with double side lighting (we used MeshLab to generate the images). Figure 4 also shows the normal images (on the right side), which consist of the mesh colored with the normal vector of each vertex.

As we can see in Fig. 4 our method obtained results whose accuracy is similar to those obtained using KinFuLargeScale. For this data-set, our scene representation required 4.27 MB (including texture), while, the $512 \times 512 \times 512$ floating TSDF volume alone requires 536 MB. In this example, our method obtained similar results with KinFuLargeScale, but our method required at least 100 times less memory. On the other hand, we observe that our method could not reconstruct all the parts of the scene. This is because we only detect planes to build the 3D scene.

To illustrate the usefulness of combining both depth and color images, we captured a large scene called *Room1* containing parts that do not have rich geometric features. Fig. 5 shows an example of RGB-D images without rich geometric features in the sequence. In such a case using depth alone fails, as shown in Fig. 6 (b). However, by combining both depth and color images, as expected, we could successfully track the camera and reconstruct the 3D scene using the frame-to-global-model strategy as shown in Fig. 6 (a). Results obtained using KinFuLargeScale with a similar camera motion are shown in Fig. 7 (c). Tracking failed when RGB-D images do not have rich geometric features, and the

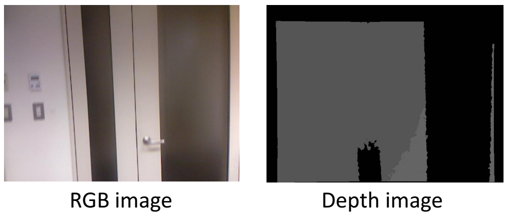

Figure 5. One input RGB-D image of the data-set *Room1*.

reconstruction stopped prematurely. The obtained reconstructed scene with our method was of 1532 K vertices and 2423 K faces and our scene representation required 34 MB. The RGB-D image sequence was processed at 2.4 fps in average when using SIFT for camera tracking, and at 7.3 fps in average when using depth only.

Results obtained with another scene called *Room2* are shown in Fig. 7 (b), (d) and in Fig. 8. In this experiment, we illustrate one interesting output of our scene representation. That is, more than 3D meshes, our method directly outputs roughly segmented 3D meshes. Therefore, we can easily remove some parts of the reconstructed scene directly after reconstruction; this enriches possible usage of our method as seen below. The example shown in Fig. 8 was obtained by simply hiding mesh layers in MeshLab. As we can see it becomes easy to remove undesired objects from the reconstructed scene (see Fig. 8 (d)), or on the contrary to keep only objects of interest (see Fig. 8 (c)). We remark that, like data *Room1*, KinFuLargeScale failed to reconstruct the scene as parts of the sequence did not have rich geometric features. Note that with the *Room2* data we observed that about 10% of points were missing because of non-planarity.

A possible usage of our scene representation is for the operation of cleaning or repairing the reconstructing scene. By using standard 2D painting softwares such as Photoshop, it is easy to edit the Bump, Mask and Color images of different planes that compose the scene. For example, the ground always contains holes because objects lying on it hide some parts. By simply in-painting the Bump, Color and Mask images, it is possible, in a post-process to fill the holes and obtain a complete mesh for the ground. In the same manner, it is also possible to remove outliers by putting their mask value to 0.

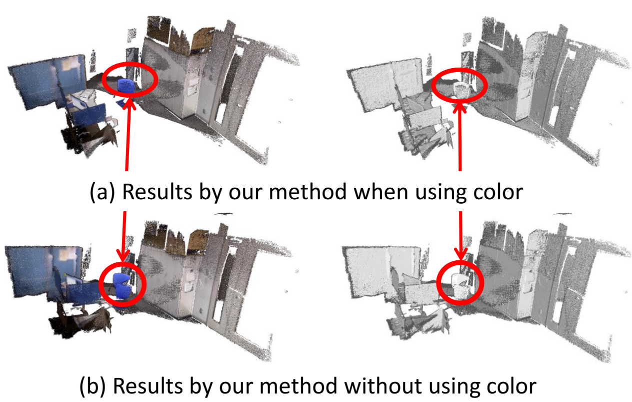

Figure 6. Results obtained with our method for the data-set *Room1* with and without using color for the camera motion tracking.

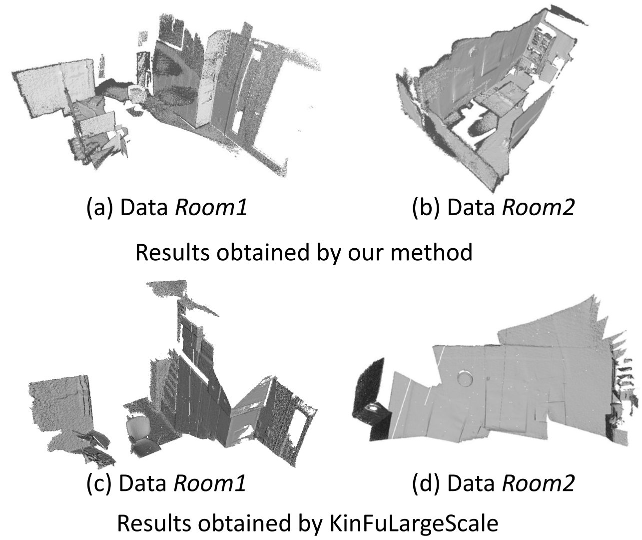

Figure 7. Results obtained by our method and KinFuLargeScale.

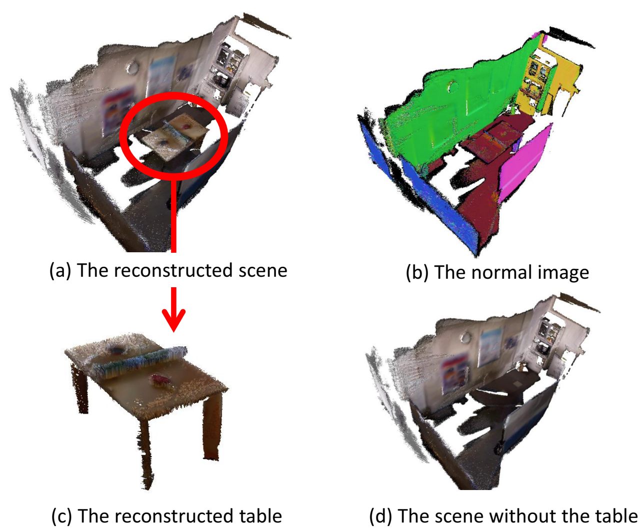

Figure 8. Results obtained with our method for the data-set *Room2*.

Figure 9 shows an example where parts of the sequence have neither geometric nor color features. As we can see in Fig. 9 (a), the reconstruction failed when reconstructing the scene as it is. But, as shown in Fig. 9 (b), by putting a few boxes on the ground we could successfully track the camera and obtain a correct reconstruction with the additional objects. Note that both image sequences were captured along similar path (*i.e.* parts of the image sequences

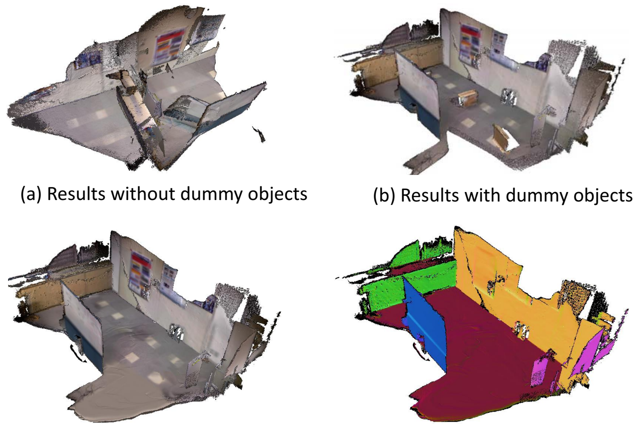

(a) Results without dummy objects (b) Results with dummy objects

(c) Results after editing ground attributes (d) Normal image

Figure 9. Results obtained for a sequence that contains parts without either rich geometric or color features.

have neither geometric nor color features). After editing the Bump, Mask and Color images of the plane corresponding to the ground we could obtain the original scene even though it was featureless, as shown in Fig. 9 (c) and (d).

6. Conclusions

We proposed a new 3D scene representation using a set of planes that achieves accurate and efficient 3D reconstruction of an indoor scene from an RGB-D image sequence, even when the scene has poor geometric features. By projecting the scene onto different planes of the scene, we introduced attributes to each plane in the scene, with which we can reduce significantly the size required for the scene representation and thus we can generate a global textured model that is light in memory use and, nevertheless, accurate and easy to update with live RGB-D measurements. In this paper, we focused only on planes to represent the scene, however, our approach can be directly applied to other parametric shapes such as spheres and even to a combination of parametric shapes. Our low memory-required representation allows to effectively use the GPU memory for other operations such as SIFT-GPU.

References

[1] KinFu Large Scene code: `http://pointclouds.org/documentation/tutorials/using_kinfu_large_scale.php`. 3, 6

[2] SIFT-GPU code: `http://www.cs.unc.edu/~ccwu/siftgpu/`. 5, 6

[3] P. Besl and N. McKay. A method for registration of 3-d shapes. *IEEE Trans on PAMI*, 14(2):239–256, 1992. 2

[4] D. Borrmann, J. Elseberg, K. Lingermann, and A. Nuhter. The 3d hough transform for plane detection in point clouds: A review and new accumulator design. *3D Research 02*, pages 1330–1332, 2011. 3

[5] E. Candes, X. Li, Y. Ma, and J. Wright. Robust principal component analysis? *Journal of the ACM*, 58(3):11:1–11:37, 2011. 3

[6] J. Chen, D. Bautembach, and S. Izadi. Scalable real-time volumetric surface reconstruction. *ACM Transaction on Graphics - SIGGRAPH'13*, 32(4):1132:1–113:8, 2013. 3

[7] T. Cormen, C. Leiserson, R. Rivest, and C. Stein. Introduction to algorithms, sec. 26.2, "the floyd-warshall algorithm". *MIT Press and McGraw-Hill*, pages 558–565, 2001. 3, 4

[8] A. Davison, I. Reid, N. Molton, and O. Stasse. Monoslam: Real-time single camera slam. *IEEE Trans. on PAMI*, pages 1052–1067, 2007. 1

[9] P. Henry, D. Fox, A. Bhowmik, and R. Mongia. Patch volumes: Segmentation-based consistent mapping with rgb-d cameras. *Proc. of International Conference on 3D Vision (3DV'13)*, 2013. 3

[10] P. Henry, M. Krainin, E. Herbst, X. Ren, and D. Fox. Rgb-d mapping: Using depth cameras for dense 2d modeling of indoor environments. *Proc. of International Symposium on Experimental Robotics*, 2010. 1, 5

[11] T. Jaeggli, T. Konenckx, and L. Gool. Online 3d acquisition and model integration. *Proc. of Procam'03*, 2003. 1

[12] M. Kazhdan, M. Bolitho, and H. Hoppe. Poisson surface reconstruction. *Proc. of Eurographics Symposium on Geometry*, 2006. 1

[13] R. Newcombe, S. Izadi, O. Hilliges, D. Molyneaux, D. Kim, A. Davison, P. Kohli, J. Shotton, S. Hodges, and A. Fitzgibbon. Kinectfusion: Real-time dense surface mapping and tracking. *Proc. of ISMAR'11*, pages 127–136, 2011. 1, 2, 5

[14] C. Nguyen, S. Izadi, and D. Lovell. Modeling kinect sensor noise for improved 3d reconstruction and tracking. *Proc. of 3DIM/PVT'12*, pages 524–530, 2012. 1, 2

[15] H. Pfister, M. Zwicker, J. Baar, and M. Gross. Surfels: Surface elements as rendering primitives. *In ACM Transactions on Graphics (Proc. of SIGGRAPH'00)*, 2000. 1, 2

[16] H. Roth and M. Vona. Moving volume kinectfusion. *Proc. of BMVC*, 2012. 1, 3

[17] A. Segal, D. Haehnel, and S. Thrun. Generalized-ICP. *Robotics: Science and Systems*, 2009. 2, 5

[18] R. Shnabel, R. Wahl, and R. Klein. Efficient ransac for point-cloud shape detection. *Computer Graphics Forum*, 26(2):214–226, 2007. 3

[19] R. Vidal, Y. Ma, and S. Sastry. Generalized principal component analysis (gpa). *Proc. of CVPR'03*, pages 621–628, 2003. 3

[20] T. Weise, T. Wismer, B. Leibe, and L. Gool. In-hand scanning with online loop closure. *Proc. of ICCV Workshops'09*, pages 1630–1637, 2009. 2

[21] T. Whelan, J. McDonald, M. Kaess, M. Fallon, H. Johansson, and J. Leonard. Kintinuous: Spatially extended kinectfusion. *Proc. of RSS Workshop on RGB-D: Advanced Reasoning with Depth Camera*, 2012. 1, 3

[22] M. Zeng, F. Zhao, J. Zheng, and X. Liu. Octree-based fusion for realtime 3d reconstruction. *Transaction of Graphical Models*, 75(3):126–136, 2013. 3

[23] Q.-Y. Zhou and V. Koltun. Dense scene reconstruction with points of interest. *ACM Transaction on Graphics - SIGGRAPH'13*, 32(4):112:1–112:8, 2013. 3